Received May 2001
Accepted October 2001

Natural convection inside dome shaped enclosures

Subrat Das and Yos Morsi
Modelling and Process Simulation Research Group, School of Science and Engineering, Swinburne University of Technology, Hawthorn, Victoria, Australia

Keywords *Natural convection, Enclosures, Finite element method*

Abstract *In the present paper the analysis of heat transfer and free convective motion have been carried out numerically for dome shaped enclosures. The solution method is based on the finite element technique with the frontal solver and is used to examine the flow parameters and the heat transfer characteristics inside dome shaped enclosures of various offsets. In formulating the solution a general conic equation is considered to represent the dome of circular, elliptical, parabolic and hyperbolic shapes. The numerical results indicate that the circular and elliptical shapes of dome give higher heat transfer rate and offset of the dome effects convective heat transfer quite significantly. However, beyond 0.3 top dome offset, the change in overall heat transfer rate is not significant. In addition, the convective phenomenon influenced by a dome shaped cover results in establishing a secondary core region even at a moderate Rayleigh number when compared with an equivalent rectangular enclosure. A good comparison between the present numerical predictions and the previous published data is achieved.*

Nomenclature

E = Offset (height of dome from top of the isothermal wall)
e = Eccentricity
g = Acceleration due to gravity, M/s^2
H = Height of the enclosure, m
h = Coefficient of heat transfer, W/m^2K
L_{ref} = Characteristic length m
n = Outward flux normal to boundary
$\bar{N}u$ = Nusselt number
p = Dimensionless fluid pressure
Pr = Prandtl number
Ra = Rayleigh number
T = Dimensionless fluid temperature
u,v = Dimensionless velocity components In x and y directions, respectively.
x,y = Dimensionless coordinates

Greek Symbols
α = fluid thermal diffusivity
β = Coefficient of volumetric expansion, $°C^{-1}$
ν = Fluid kinematic viscosity, m^2/s
ρ = Fluid density, Kg/m^3
γ = Aspect ratio

Subscript
h,c = Hot and cold wall, respectively

1. Introduction

Even after 40 years of research on the fluid flow and transport processes generated or altered by buoyancy forces in enclosures, most of the investigations found in the literature are related to regular shapes such as square, rectangular, cylindrical, annulus etc. However, almost in all practical

International Journal of Numerical Methods for Heat & Fluid Flow, Vol. 12 No. 2, 2002, pp. 126–141.

DOI 10.1108/09615530210418294

applications including solar heating, nuclear waste disposal, solidification, preservation of food grains, drugs and other granular products irregular shaped enclosures are utilized. Due to the complexity of natural convection problem in non-rectangular and non-cylindrical type of enclosures particularly curved boundary enclosures, very few studies have been found in literature. These and other published investigations that are considered to be of relevance to the present investigation are briefly reviewed in the next section.

The review carried out by Hoogendoorn (1986) and later Ostrach (1988) have highlighted the complexity of the numerical solutions of the nature convection problems inside enclosures. Later various investigations on the analyses of laminar natural convection in different enclosures including parallelogram, trapezoidal, triangular and other non-rectangular shaped were reported. (Akinsate and Coleman (1982); Campo *et al.* (1988); Evren-Selamet *et al.* (1992); Moukalled and Acharya (1997); Volkers *et al.* (1996); Ramaswamy and Moreno (1997), Das and Sahoo (1998)). Moreover, recently Holtzman (2000) have investigated natural convection within isosceles triangular enclosure with heated bottom horizontal wall.

With respect to the curved wall enclosures, considerable attention has been given to the effect of convective heat transfer due to the curved wall since the work of Kaviany (1984). Kaviany reported the effects of semicylindrical shaped protuberance, located at the bottom cavity, on total and local heat transfer rates. His findings show that the presence of protuberance leads to a decrease in heat transfer rates in the lower part of the enclosure. Experimental investigations related to curved irregular enclosures include the work of Lewandowski *et al.* (1992) and Asfia *et al.* (1996). Later Lewandowski *et al.* (1998) however, investigated numerically the heat transfer and free convective motion inside enclosures of different hemispherical convex or concave shapes. The findings from these studies indicated that the presence of the hemispherical bottom has the most inhibitory influence on convective heat transfer. Moreover, the authors have shown that the continuity of the boundary layer is broken on the convexity of the bottom and transforms into a plume and mixes the entire volume of the fluid, thus intensifying the heat exchange. In addition they also discussed various effects due to the dead space, variation of boundary layers and local heating, which significantly affect the natural convection phenomena within the enclosure. Very recently Laouadi and Atif (2001) have reported another numerical investigation on the natural convection phenomena within a dome shape enclosure having a hemispherical cup. The authors reported that the prediction of heat transfer has been very difficult due to complex flow patterns that vary with geometry parameters and boundary conditions. They also found that the convective heat transfer for fully hemisphere domes to be remarkably high. Another study worthy of noting is the work of Gadoin *et al.* (2001) who investigated the flow instabilities within

complex enclosures and discussed the general methodology for studying instabilities of natural convection flows in cavities of complex geometry.

The above discussion has highlighted the effect of the interaction between the boundary layer and core region, which can result in introducing several complexities, and is inherent to all confined convection configurations. Moreover, it is recognized that the core flow is so sensitive to the geometry as well as the boundary conditions and hence the fluid flow phenomena cannot be predicted a priori from the given adhoc boundary conditions. Moreover, in cases of inclined/curvature boundaries the situation is even more intricate because there may be more than one global core and flow sub-regions possible, such as cells and layers embedded in the core. However, there is a need to develop a comprehensive model capable of analyzing the effect of irregular shapes quantitatively. In particular the effect of a curved boundary wall on convective flow and heat transfer is not fully understood. Therefore in this paper we are mainly interested in generalizing the problem by considering the dome of circular, elliptical, parabolic and hyperbolic shapes under various operating conditions.

2. Problem definition and governing equations

Here a two-dimensional steady-state analysis of an incompressible fluid, driven by the buoyancy force is examined for various dome enclosures. The governing equations considered here are same as that of De Vahl Davis (1983). Using the Boussinesq approximation and neglecting the dissipation effect due to the viscous term and no heat generation, the governing equations in non-dimensional form are written as follows:

$$\frac{\partial u}{\partial x} + \frac{\partial v}{\partial y} = 0 \tag{1}$$

$$u\frac{\partial u}{\partial x} + v\frac{\partial u}{\partial y} = -\frac{\partial p}{\partial x} + Pr\left[\frac{\partial^2 u}{\partial x^2} + \frac{\partial^2 u}{\partial y^2}\right] \tag{2}$$

$$u\frac{\partial v}{\partial x} + v\frac{\partial v}{\partial y} = -\frac{\partial p}{\partial y} + Pr\left[\frac{\partial^2 v}{\partial x^2} + \frac{\partial^2 v}{\partial y^2}\right] + TRaPr \tag{3}$$

$$u\frac{\partial T}{\partial x} + v\frac{\partial T}{\partial y} = \frac{\partial^2 T}{\partial x^2} + \frac{\partial^2 T}{\partial y^2} \tag{4}$$

Equations (1–4) were normalized using the following dimensionless scales

$$(x, y) = (x^*, y^*)/L_{\text{ref}}; \qquad (u, v) = (u^*, v^*)L_{\text{ref}}/\alpha; \qquad p = p^* L_{\text{ref}}^2/(\rho\alpha^2);$$

$$T = (T^* - T_c)/(T_h - T_c); \qquad Ra = g\beta(T_h - T_c)L_{ref}^3/(\nu\alpha); \qquad Pr = \nu/\alpha;$$

Where asterisks denote dimensional variables.

In obtaining the numerical solution of the dome shaped enclosure, the following boundary conditions and the flow domain as illustrated in Figure 1 were used. On surface of I $u = v = 0$; $T_h = 1$. On surface of II & IV $u = v = 0$; $\partial T/\partial n = 0$. On surface of III $u = v = 0$; $T_c = 0$.

3. Computational domain

The model configuration and coordinate (x,y) system are shown in Figure 1 which represents a typical dome shaped enclosure. The general conic equation to represent the top dome shape is given by

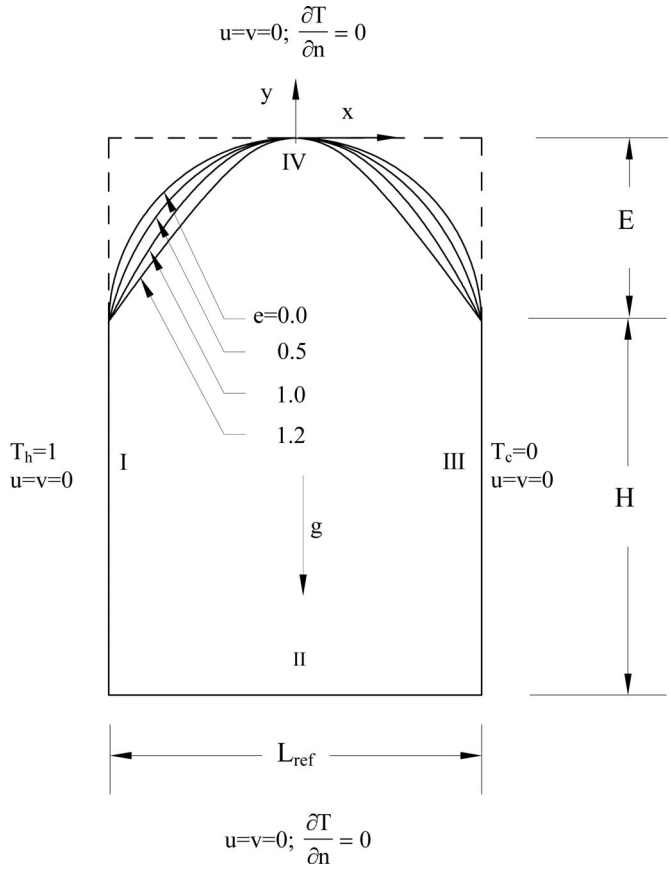

Figure 1.
Coordinate system

$$(1-e^2)y^2 + 2\left[\frac{(1-e^2)E}{2} + \frac{1}{8E}\right]y + x^2 = 0 \tag{5}$$

where $E = E^*/L_{\text{ref}}$ ('offset') is introduced to recast equation (5) in dimensionless form, and e is defined as eccentricity of the curvature boundary which decides the shape of the top adiabatic cover depending upon the values as given below. $e = 0$ for Circular; $0 < e < 1$ for Elliptical; $e = 1$ for Parabolic; $e > 1$ for Hyperbolic.

As previously discussed these shapes of enclosures have become increasingly popular in various engineering applications particularly in modern building design and most importantly in the area of storage of grains, drugs and other granular products.

4. Solution procedure

Equations (1)–(4) result in a set of non-linear coupled equations for which an iterative scheme is adopted. The total domain is discretised into 340 elements that results in 1083 nodes. All the elements are isoparametric, quadrilateral containing eight nodes. All eight nodes are associated with velocities as well as temperature; only the corner nodes are associated with pressure. This is an accepted practice of depicting the variation in pressure by a shape function, which has one order less than those defining velocities and temperature (Taylor and Hood, 1973).

A suitable element numbering scheme as proposed by Sloan (1989) is adopted so as to achieve an optimal front width of 140 for the given geometry of the model and subsequently the frontal solver is used to solve the above set of equations. The advantage of using the frontal solver is in that of core memory requirement and is much less than general conventional banded solver.

5. Presentation and discussion of results: validation of the current method

In validating the current numerical scheme an enclosure having two differentially heated vertical isothermal walls ($T_{\text{h}} = 1, T_{\text{c}} = 0$) and two horizontal adiabatic walls. The range of aspect ratio, γ, considered here is 1 ($H = L_{\text{ref}}$) to $1 + E$. The no-slip condition is applied to all boundary walls for the validation of the numerical procedure and comparison with the dome shaped enclosure. Maximum value of Rayleigh number, i.e. $Ra = 10^6$, was used. The predicted quantities of average Nusselt number, $\bar{Nu}$, on the hot wall and maximum vertical velocity, $v_{\max}$ have been compared with the benchmark numerical solutions of De Vahl Davis (1983) and Tabbarok and Lin (1977), Table I. It may be noted that De Vahl Davis obtained the solution, based on finite difference method using rectangular mesh whereas Tabbarok and Lin (1977) used finite element method based on stream-vorticity formulation. The results obtained in the present numerical scheme also have been compared with

	$Ra = 10^3$		$Ra = 10^4$		$Ra = 10^5$		$Ra = 10^6$		Grashof No. $= 10^3$		Grashof No. $= 5 \times 10^3$		Grashof No. $= 10^4$	
	Present	De Vahl Davis	Present	De Vahl Davis	Present	De Vahl Davis	Present	De Vahl Davis	Present	Tabbarok & Lin	Present	Tabbarok & Lin	Present	Tabbarok & Lin
$\bar{N}u$	1.122	1.116	2.243	2.238	4.523	4.509	8.828	8.817	1.068	1.068	1.605	1.653	2.029	2.108
V_{max}	7.86	–	19.60	19.617	68.52	68.59	220.81	219.36						

Table I.
Comparison of present results with De Vahl Davis (1983) & Tabrok and Lin (1977)

the predicted results of $\bar{Nu}$, in Table I. It is observed that the present results are in good agreement with previous published data and the minor differences are attributed to either the different numerical scheme or the grid adopted in the concerned studies.

6. Numerical results of dome shaped enclosures

Numerical results were obtained for various parameters such as Rayleigh number, Ra, offset, E and eccentricity, e. The range of these parameters are $1 \leq Ra \leq 4 \times 10^4$, $0.1 \leq E \leq 0.5$ and $0 \leq e \leq 1.2$ respectively. The eccentricity, e, here indicates the nature of the dome and presumes typical value of 0.0, 0.5. 1.0 and 1.2 for circular, elliptical, parabolic and hyperbolic top conic section, respectively.

The offset measures the height of the dome from the isothermal walls. Note that the square enclosure with aspect ratio unity indicates that the height of the isothermal wall is equal to the width of the enclosure. However, a dome shaped enclosure with offset E is equivalent to an aspect ratio of $1 + E$ for the corresponding rectangular enclosure having the height, $1 + E$.

7. Temperature and velocity fields

The isotherms and streamlines are plotted in Figure 2(a). It can be seen that the temperature gradient is negative along the x direction, giving rise to clockwise unicellular rotation at the central part of the domain. However, an increase in Rayleigh number results in the dominance of convective current. This is evident from the large temperature gradient near the hot and cold isothermal walls. With further increase in Rayleigh number, the gradient of temperature is changed to zero or positive at the central part of the domain, which results in a secondary vorticity in the core region. In addition, the streamlines at the bottom of the enclosure found to be more densely packed than the top ones. This indicates that the resultant flow velocity at the bottom of the enclosure is more predominant than that at the top due to the geometry of the enclosure.

There is a reduction in the u-velocity in the central part of the domed boundary. This is due to the fact that the flow gets a larger surface area due to dome shape while passing from the top hot corner to the top central part of the enclosure and gently deflecting over the curved top cover near the hot wall. This results in a weakening of the vorticity near the wall. This weaker vorticity near the wall may not able to sustain a weak return motion of fluid near the cold wall. Therefore, due to the weakening of u-velocity, the core flow is disturbed to give rise to a secondary vorticity in the central part of the domain even at a moderate range of Rayleigh numbers.

The contour plots of $u-v$ velocities are shown in Figure 2(b), The peak u-velocities are observed at the top and bottom parts of the enclosure and as Rayleigh number increases these velocities shift to the top of the hot wall and bottom of the cold wall. A similar situation also prevails for peak v-velocities

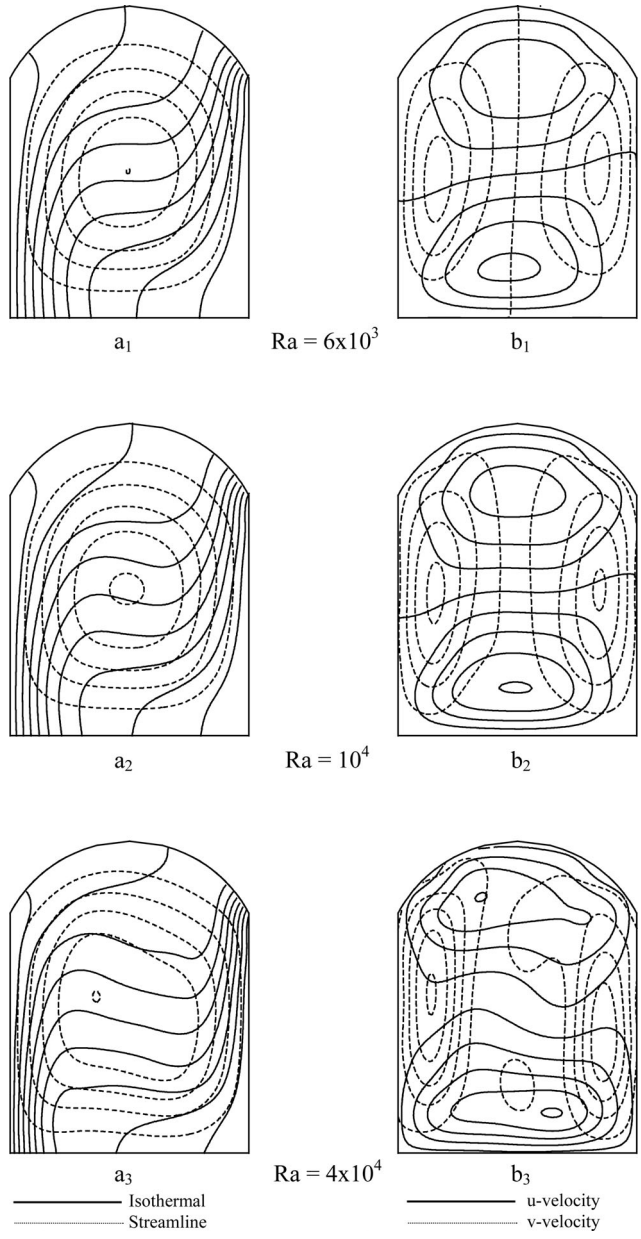

Figure 2.
Comparison of isotherms & streamlines and $u-v$ velocities for different Rayleigh numbers ($Pr = 1$) at $E = 0.3$, $e = 0.0$

that occur at the sides of the isothermal walls and again with the increase in Rayleigh number these velocities shift similarly. These two velocity components give the resultant velocities, which reveal the peaks at the top of the hot wall and at the bottom of the cold wall. Moreover, due to the buoyancy

force effect, it is evident from the contour plots that the v-velocity always remains dominant over the u-velocity at the isothermal walls. Note that the contour plots of the u-velocity clearly distinguish the effect of the circular top and the flat bottom. The streamlines results show a large velocity gradient at the wall, which in turn results in a severe temperature gradient as well.

In Figures 3 and 4, the u-velocity at the mid vertical axis and the v-velocity at the axis of the mid isothermal walls confirms the clockwise unicellular flow through out the enclosure. A comparison of velocities of each dome shaped enclosure is made with its equivalent square and rectangular enclosures as depicted in the same Figures 3 and 4 respectively. It is observed the u-velocity deviates a lot from its symmetry and this may be attributed to the effect of top dome shape cover. It is also observed that for the same offset, the different curvature of the dome yields different velocities in the upper half, while the difference is not appreciable in the lower half due to flat bottoms of all the enclosures.

Moreover, it should be also noted that the v-velocity in Figure 4, is almost symmetrical about the mid-horizontal axis. When the dome shaped enclosures are compared with square and equivalent rectangular enclosure, it is observed that the v-velocity is comparatively higher at higher Rayleigh number. This is mainly due to the curved adiabatic top cover, which permits a smooth passage to fluid near the top corner of the hot wall. However, when the fluid enters the dome shaped area it decelerates substantially resulting lower u-velocity in the top central part of the dome. This is considered to be the basis why the u-velocity is substantially low at the top central part than that of a square or equivalent rectangular enclosures.

8. Heat transfer results

In the case of the horizontal top cover, low heat transfer rates are expected to exist due to the severe deflection of flow away from the vertical walls. However, the domed shape top cover allows the convective current more smoothly over the curved surface, which enhances the heat transfer rate from the hot wall when compared with the square enclosure.

Moreover, the dome shaped top cover influence the convective flow to an extent that a pure conduction region never prevails even at a very low Rayleigh number. There is bound to be certain amount of convection due to the curved top adiabatic wall even at a very low Rayleigh number. This is the reason why an enclosure having a curved wall may experience the onset of convection at a lower range of Rayleigh number as compared to that of rectangular enclosures. The increase in offset, E improves the convective currents, therefore, a net rise in the mean heat transfer rate along the hot wall is expected and is observed. However, dome shaped enclosures proved to be less efficient in terms of heat transfer rate when compared with the equivalent rectangular enclosure

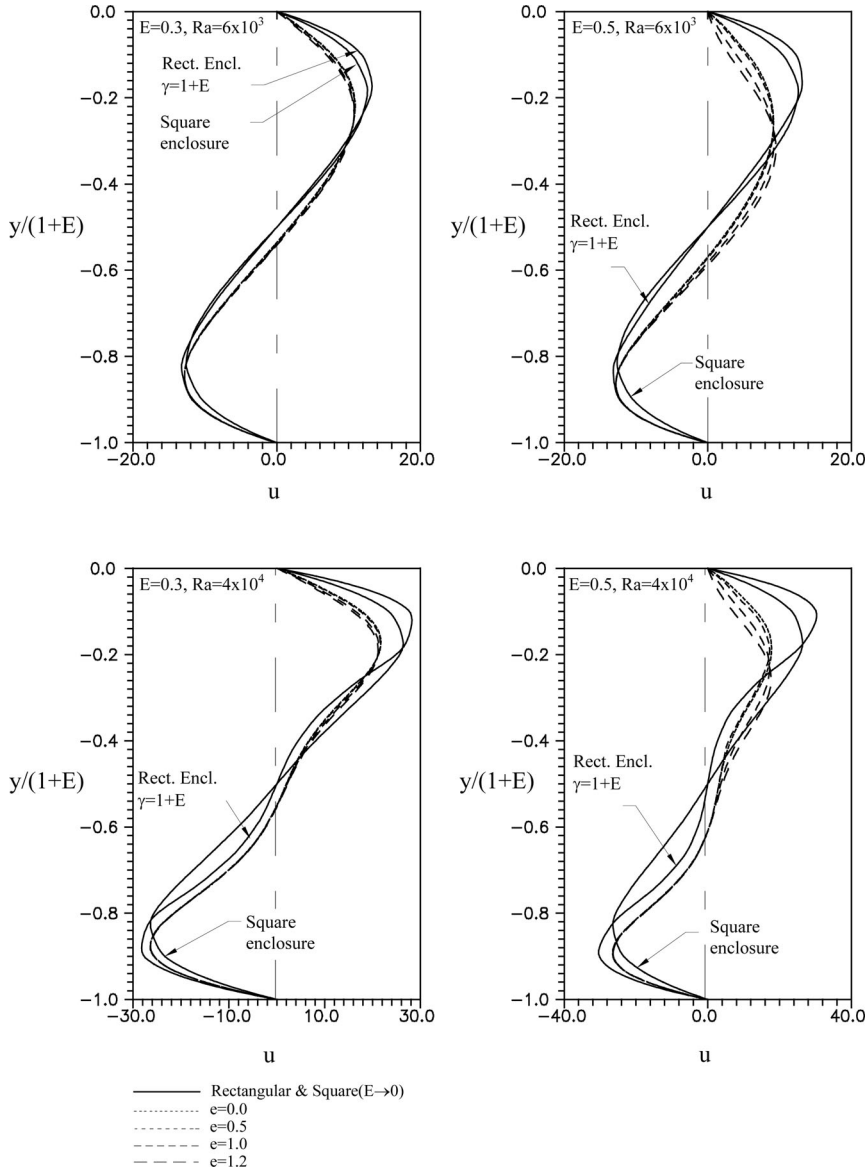

Figure 3.
Non-dimensional *u*-velocity profile at the mid-vertical axis

because of less heat transfer area along the hot isothermal wall, as shown Figure 5.

9. Nusselt number calculation

Nusselt number for the isothermal wall of the enclosure is derived from the energy balance equation as follows

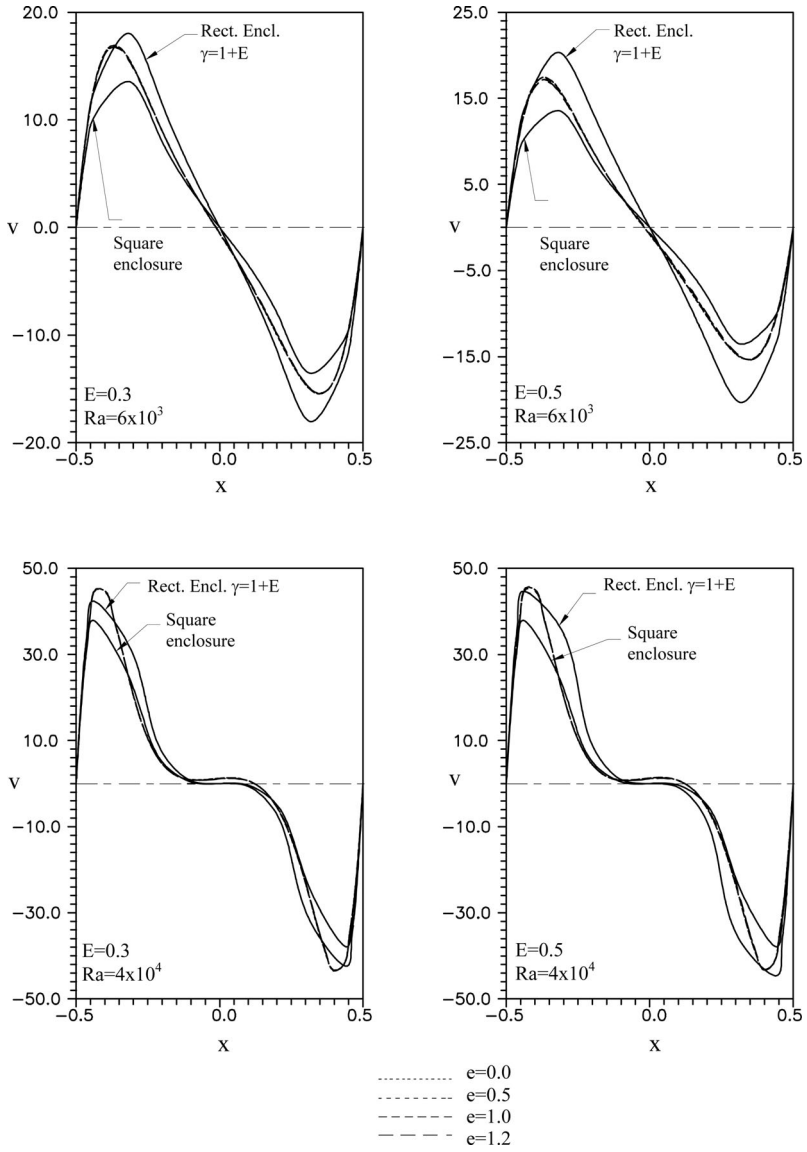

Figure 4.
Non-dimensional v-velocity profile at the mid horizontal axis of the isothermal walls

$$\bar{N}u = \frac{hL_{ref}}{k} = -\frac{\partial T}{\partial n} \tag{6}$$

The average Nusselt number over the total length of the hot wall is

$$\bar{N}u = \frac{1}{L_{ref}} \int_0^L -\frac{\partial T}{\partial n} \mathrm{d}n \tag{7}$$

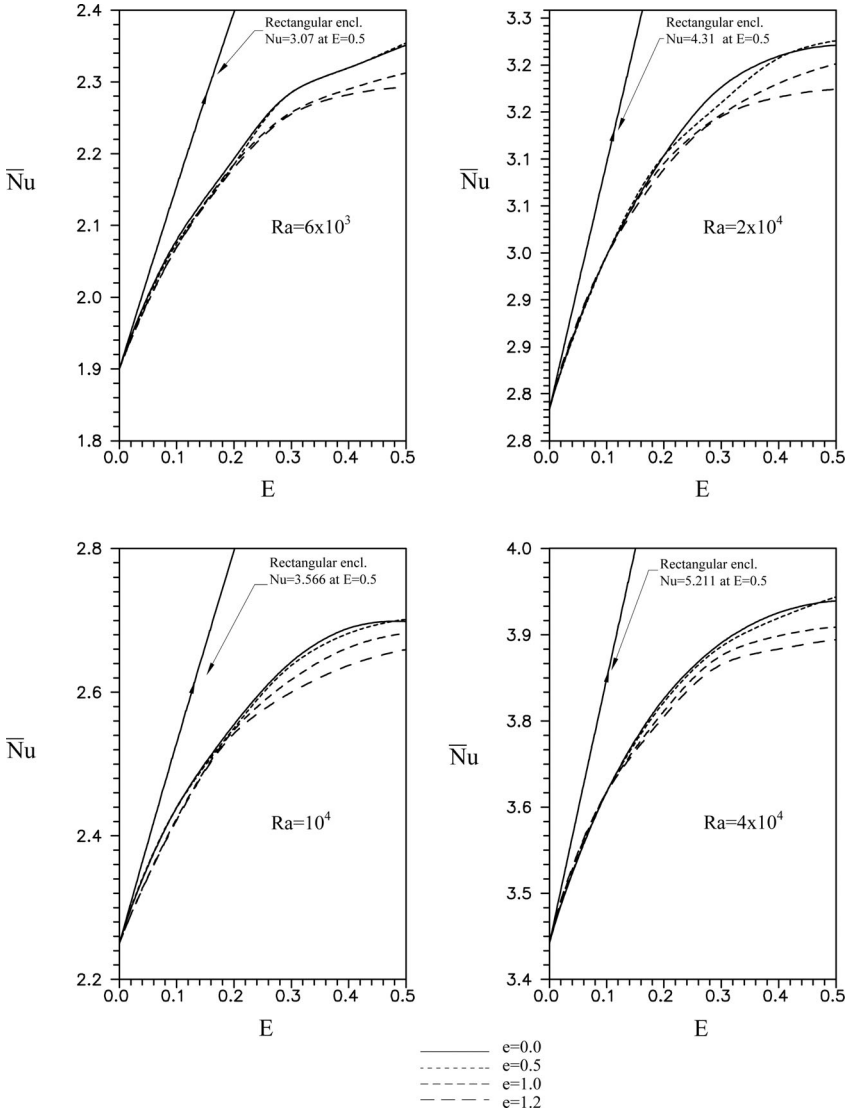

Figure 5.
Comparison of Nusselt number for the dome, square and rectangular enclosures with different values of offset, *E*

Nusselt number is also plotted for all type of conic sections such as circular, elliptical, parabolic and hyperbolic top adiabatic dome covers at different offsets, Figure 5. The most interesting results to be noted is that an increase in offset beyond 0.3 for all conic sections, brings stagnation in the improvement of convective current near the hot wall which indicates no significant increase in

Ra	$\bar{Nu}$ $e = 0.0$	$e = 0.5$	$e = 1.0$	$e = 1.2$
$E = 0.1$				
6×10^3	2.080	2.080	2.070	2.070
8×10^3	2.265	2.265	2.265	2.264
10^4	2.440	2.440	2.427	2.422
2×10^4	2.987	2.987	2.987	2.987
4×10^4	3.661	3.661	3.661	3.661
$E = 0.2$				
6×10^3	2.190	2.190	2.190	2.180
8×10^3	2.393	2.393	2.380	2.380
10^4	2.555	2.550	2.547	2.542
2×10^4	3.114	3.114	3.104	3.097
4×10^4	3.791	3.790	3.773	3.766
$E = 0.3$				
6×10^3	2.285	2.285	2.258	2.255
8×10^3	2.475	2.470	2.453	2.450
10^4	2.642	2.637	2.617	2.600
2×10^4	3.201	3.182	3.167	3.164
4×10^4	3.869	3.863	3.851	3.838
$E = 0.4$				
6×10^3	2.320	2.320	2.290	2.283
8×10^3	2.522	2.522	2.495	2.472
10^4	2.689	2.682	2.662	2.637
2×10^4	3.241	3.239	3.207	3.189
4×10^4	3.911	3.903	3.878	3.861
$E = 0.5$				
6×10^3	2.351	2.354	2.312	2.292
8×10^3	2.551		2.522	2.490
10^4	2.698	2.701	2.682	2.660
2×10^4	3.255	3.261	3.231	3.200
4×10^4	3.927		3.891	3.873

Table II.
Average Nusselt Number at the hot wall for different offsets and eccentricity

the mean Nusselt number. However, for the circular top cover ($e = 0.0$), the percentage rise in Nusselt number in the lower offset (i.e. 0.1 to 0.2) is about 5.02 and only 1.2 at higher offset (0.4 to 0.5), see Table II. It is also observed that an increase in offset (> 0.3) for all types of conic sections, resulting in lower velocity, which is the important contributing factor affecting the improvement of convective heat transfer.

The effect of different curvatures of the domed shape cover is also shown at a varying Rayleigh numbers in Figure 6. These curvatures have little effect on the mean Nusselt number at a very low value of offset, even at the highest range of Rayleigh number. However, at higher offsets and at high Rayleigh

numbers, it is found that the circular and elliptical curvatures have the most significant effect on the convective heat transfer compared to other curvatures as shown in Figure 6. The calculated values of mean Nusselt number have been tabulated in Table II for different Rayleigh number, eccentricity and offset values.

The tabulated value show that the relative increase in convective heat transfer becomes more pronounced in the lower range of E, offset (0.1–0.2), but become less significant as the offset increases beyond 0.3.

10. Conclusion

The present numerical scheme is validated for accuracy in the prediction of buoyancy driven flow within enclosures having curvature boundary. The predicted results show that domed shape enclosures have a significant effect on the convective flow and heat transfer characteristics. Hence the character of the curvature of the enclosure must be incorporated in the analysis of the flow and heat transfer phenomena.

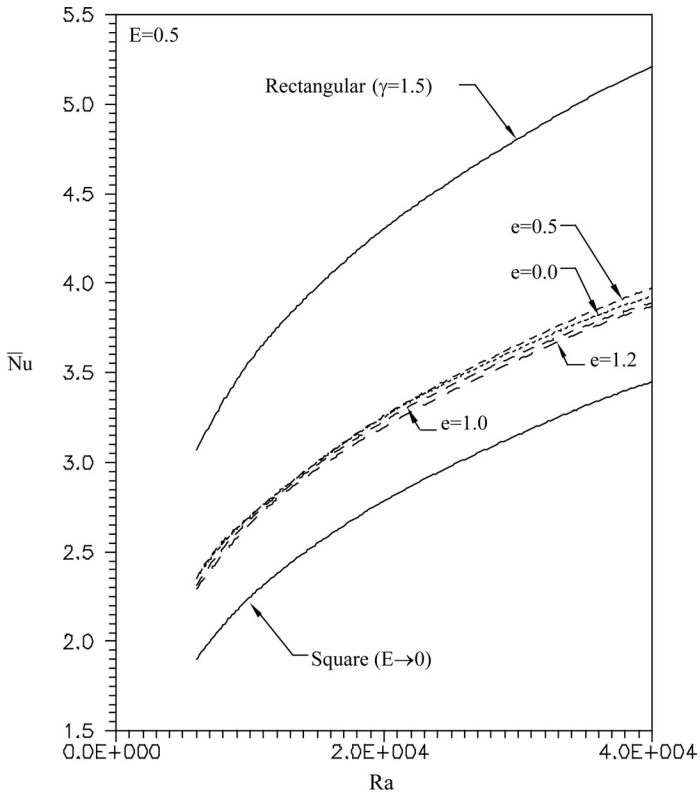

Figure 6.
Comparison of average Nusselt number for square, dome and rectangular enclosures with different Rayleigh Numbers ($Pr = 1$)

It was also found that domed shape enclosures having offset in the range of 0.25 to 0.3 have the maximum heat transfer rate for all types of conic surfaces.

References

Akinsate, V.A. and Coleman, J.A. (1982), "Heat transfer by steady state free convection in triangular enclosures", *Int. J. Heat Mass Transfer*, Vol. 25, pp. 991-8.

Asako, Y. and Nikamura, H. (1982), "Heat transfer in a parallelogram shaped enclosure", *Bull. JSME*, Vol. 25, pp. 1419-27.

Asfia, F.J., Frantz, B. and Dhir, V.K. (1996), "Experimental investigation of natural convection heat transfer in volumetrically heated spherical segments", *ASME J. Heat Transfer*, Vol. 118, pp. 31-7.

Campo, E.M.D., Sen, M. and Ramos, E. (1988), "Analysis of laminar natural convection in triangular enclosure", *Numer. Heat Transfer*, Vol. 13, pp. 353-72.

Das, S. and Sahoo, R.K. (1998), "Velocity-Pressure formulation for convective flow inside enclosure with top quadratic inclined roof", *J. Energy Heat Mass Transfer*, Vol. 20, pp. 55-64.

De Vahl Davis, G. (1983), "Natural convection of air in square cavity: A bench mark numerical solution", *Int. J. Numer. Meth. Fluids*, Vol. 3, pp. 249-64.

Everen-Selament, E., Arpaci, V.S. and Borgnakke, C. (1992), "Simulation of laminar buoyancy-driven flows in an enclosure", *Numer. Heat Transfer*, Vol. 22, pp. 401-20.

Gadoin, E., Quere, Le P. and Daube, O. (2001), "A general methodology for investigating flow instabilities in complex geometries: application to natural convection in enclosures", *Int. J. Numer. Meth. Fluids*, Vol. 37, pp. 175-208.

Holtzman, G.A. (2000), "Laminar natural convection in isosceles triangular enclosures heated from below an symmetrically cooled from above", *J. Heat Transfer*, Vol. 122 No. 3, pp. 485-91.

Hoogendoorn, C.J. (1986), "Natural convection in enclosures", *Proceedings' Eighth International Heat Transfer Conference, San Francisco*, Hemisphere publishing Corp., Washington, DC, Vol. 1, pp. 111-20.

Kaviany, M. (1984), "Effect of a protuberance on thermal convection in a square cavity", *J. Heat Transfer*, Vol. 106, pp. 830-4.

Laouadi, A. and Atif, M.R. (2001), "Natural convection heat transfer within multi-layer domes", *Int. J. Heat Mass Transfer*, Vol. 44 No. 10, pp. 1973-81.

Lewandowski, W.M. and Khubeiz, M.J. (1992), "Experimental study of laminar natural convection in cells with various convex and concave bottoms", *J. Heat Transfer*, Vol. 114, pp. 94-8.

Lewandowski, W.M., Khubeiz, J.M., Kubski, P., Bieszk, H., Wilczewski, T. and Szymanski, S. (1998), "Natural convection heat transfer from complex surface", *Int. J. Heat Mass Transfer*, Vol. 41, pp. 1857-68.

Moulkalled, F. and Acharya, S. (1997), "Buoyancy-induced heat transfer in partially divided trapezoidal cavities", *Numer. Heat Transfer, Part A*, Vol. 32, pp. 787-810.

Ostrach, S. (1988), "Natural convection in enclosures", *ASME J. Heat Transfer*, Vol. 110, pp. 1175-90.

Ramaswamy, B. and Moreno, R. (1997), "Numerical study of three-dimensional incompressible thermal flows in complex geometries, Part I: Theory and benchmark solution", *Int. J. Numer. Meth. Heat Fluid Flow*, Vol. 7, pp. 297-343.

Sloan, S.W. (1989), "A Frontal Program for Profile and Wavefront Reduction", *Int. J. Numer. Meth. Eng.*, Vol. 28, pp. 2651-79.

Tabbarok, B. and Lin, R.C. (1977), "Finite element analysis of free convection flows", *Int. J. Heat Mass Transfer*, Vol. 20, pp. 945-52.

Taylor, C. and Hood, P.A. (1973), "Numerical solution of the Navier-Stokes equations using the finite element technique", *Computer and Fluids*, Vol. 1, pp. 73-100.

Volker, S., Burton, T. and Vanka, S.P. (1996), "Finite-volume multigrid calculation of natural convection flows on unstructured grids", *Numer. Heat Transfer*, Vol. 30, pp. 1-22.